GAS BUBBLES IN THE SEA: A REVIEW AND MODEL PROPOSALS

by

Robert Bruce Williams and Leslie A. Foster
SACLANT ASW Research Centre
La Spezia, Italy

ABSTRACT

The literature pertaining to both free bubbles (Pt 1) and bubbles associated with fish anotomy (Pt 2) is reviewed with particular emphasis on their distributions in the sea and influencing factors. An attempt is made to compact the results to date into simple, mostly empirically-based models. Some of the models proposed contrast with those previously used. For example, depth dependence of free-bubble concentrations is proposed to be simply influenced by pressure, which causes a $(\text{depth})^{-2/3}$ relationship for Medwin's 1970 data (radius > 60 micrometres) for depths greater than 10 metres, while at shallower depths the dependence is less. In refitting data of fish-bladder volume to be proportional to $(\text{length})^{N}$, N was strongly dependent on the type of fish, and in all cases, N was larger than previously accepted. Finally, a free-bubble concentration-function model is proposed which is a linear sum of functions of a single generating mechanism (waves, rain, photosynthesis, etc.). Although this last step may be premature from the standpoint of our present knowledge of the subject, it supplies a basic structure and aids in clarifying where knowledge is lacking.

PART 1 FREE BUBBLES

INTRODUCTION

Knowledge of gas bubbles in the sea becomes important in many diverse subjects, which include:

Visibility in the lower atmosphere;

cloud formation due to salt particles injected into the air by bursting bubbles;

underwater acoustic-propagation characteristics such as absorption, scattering and sound-speed modification;

acoustic noise;

exchanges of properties at the air/sea interface, such as water, gases, heat, salt, and bacteria;

sea-surface chemistry, such as fractionation processes;

vertical transport of a variety of properties due to the scavenging effect of the bubbles.

Although this list is quite encompassing, relatively little work has been devoted to the study of gas bubbles in the sea and very few measurements of bubble concentration and size distributions have been made.

The first measurement of sea bubbles were those of Blanchard and Woodcock (1957), hereafter referred to as B &W, who, motivated by the problems of salt-nuclei formation in the atmosphere, made some near-beach estimates of bubble concentrations from breaking waves. Glotov et al (1962) studied bubble formation in a tank with various wind speeds. But by far the most work has come from Medwin (1970, 1974, 1975) and his associates at the Monterey U.S. Naval Post-Graduate School. His measurements range over depths of 5 to 45 ft in different sea states, different locations, and with different techniques. The purpose of this paper is to review what has been measured and what models have been put forth to date, condense this information into cohesive models that reflect the various data, and point out what information is lacking.

1. VERTICAL VELOCITY AND GAS DIFFUSION

B &W set the frictional (Stokean) drag force equal to the buoyancy force, and derived a relationship between the bubble radius, R, and the vertical velocity, w:

$$R = \frac{3}{8} \frac{C_d}{g} w^2 , \qquad \text{[Eq. 1]}$$

g being the acceleration due to gravity and C_d the spherical drag coefficient (Goldstein, 1938). They compare this with the measurements of Allen (1900) and show good agreement in the range of his measurements, $10^2\ \mu m < R < 10^3\ \mu m$.

Le Blond (1969) notes that in all but the cleanest of liquids, the vertical velocity of a gas bubble for small Reynolds numbers is given by the solid sphere formula:

$$w_d = \frac{2}{3} g \frac{R^2}{\nu} , \qquad \text{[Eq. 2]}$$

instead of the Rybezynaki-Hadamand expression for a gas sphere:

$$w_c = \frac{1}{3} g \frac{R^2}{\nu} \qquad \text{[Eq. 3]}$$

where ν is the kinetic viscosity of the liquid, and where the subscripts d and c refer to dirty and clean bubbles, respectively. The supposition is that minute particulate or organic matter forms a film around the bubble. In addition, for small Reynolds numbers, the mass flux of gas out of the bubble is given by

$$F_c = 24\left(\frac{\pi g D}{2\nu}\right)^{\frac{1}{2}} R^{\frac{1}{2}}(C - C_\infty)$$

$$F_d = 72\left(\frac{2gD^2}{9\nu}\right)^{\frac{1}{3}} R^{\frac{4}{3}}(C - C_\infty) \qquad \text{[Eq. 4]}$$

where D is the diffusivity of the gas,

C is the concentration (g/cm^3) in the bubble, and

C_∞ is the concentration far away from the bubble.

He states that Eqs. 2, 3 and 4 apply for $r < 80\ \mu m$. We note that Eq. 1 reduces to Eq. 3 with:

$$C_D = \frac{24\ \nu^2}{gR^3} .$$

Datta, et al (1950) have noted that bubbles greater than about 1 mm radius tend to zig-zag in their ascent, and that their vertical velocity may even become less than that of a slightly smaller radius. Furthermore, a plateau is reached where w remains constant for radii between 2 and 7 mm. In this region, distortions from the spherical shape are seen.

Turner (1972) has made an analysis of the deformation of large bubbles in a high Reynolds number ascent, and shows that the shape is like that of an umbrella, or a mature atomic-bomb cloud. In terms of an equivalent radius, whose volume is the same as the deformed bubble,

$$\omega = \frac{2}{3}\left(g\frac{R}{\alpha}\right)^{\frac{1}{2}}, \quad \alpha = 0.49 \pm 0.09 \ . \qquad \text{[Eq. 5]}$$

However, bubbles of this size tend to break up. Note that this is the same as Eq. 1, with $C_D = 1$.

To summarize, for small radii (< 80 μm) Eqs. 2 or 3 can be used for vertical velocity. For radii up to 1 mm, the more general equation [Eq. 1] is necessary. From 2 mm to 7 mm, it appears that the best prediction for the velocity is a constant (25 cm/s). Above a 7 mm equivalent radius, Eq. 5 must be used. Equation 4 describes the gas flux out of the bubble for small ($r < 80$ μm) bubbles. To our knowledge, there are no predictions of gas flux for larger bubbles.

2. LIFETIME OF BUBBLES

By considering only gas saturation, a bubble might be expected to lose some of its gas by diffusion and therefore its volume will be expected to diminish if the sea is undersaturated while a bubble in supersaturated water would be expected to grow. However, additional factors need to be included to predict the evolution of a bubble. B & W have extended the calculations of Wyman et al (1952) regarding the rate of growth of a bubble, taking into account the surface tension effects, which are of prime importance for small bubbles. Figure 1 shows these lifetime calculations vs bubble diameter for different saturation percentages at 10 cm depth. The result is that for a given supersaturation there exists a depth below which bubbles of any radius will go into solution. That depth is simply given by

$$d = 10\ (x-1) \text{ metres} \qquad \text{[Eq. 6]}$$

where x is the fraction of saturation. Thus, for example, all bubbles deeper than 1 metre will go in solution in 110% super-saturated waters.

Turner (1961) found that, in laboratory experiments, small bubbles can persist for long periods of time, or indefinitely in apparent contradiction to the results of B & W. However, he attributes this persistence to particulate matter in the water, possibly forming "walls" around the bubble so as to support excess pressure and block gas diffusion. Even small amounts of particulate matter in the water produced lifetimes greater than 100 hours.

Le Blond (1969) studies theoretically the problem of gas diffusion in an ascending bubble. He points out that even in subsaturated water a bubble may grow in volume provided its ascending velocity is large enough so that the ambient pressure decreases faster than the pressure reduction due to loss of gas by diffusion.

His model predicts the existences of two critical radii: r_a, above which the volume will grow; and r_b, below which the gas pressure increases while the volume shrinks and ultimately collapses. The fate of bubbles whose radii lie in between r_a and r_b cannot be easily predicted from his model, but must either ultimately grow or collapse.

For velocities in the Stoke's regime, Le Blond has explicit expressions for r_a and r_b:

$$r_a = \left[\frac{3\nu}{\alpha g}\,\beta_c (P - \gamma)\right]^{2/5}$$

$$r_b = \left(\frac{2\sigma}{3P}\right)^{2/7} r_a^{\,5/7} \qquad \text{[Eq. 7]}$$

$$\gamma = \frac{C_\infty}{K}\,, \quad \beta_c = 8\left(\frac{\pi g D}{2\nu}\right)^{\frac{1}{2}} K$$

where the coefficient of absorption (Dorsey 1940, p.529), $K = \frac{C}{P}$. C is the concentration of gas in the liquid at the gas-liquid interface, P the pressure inside the bubble and σ the surface tension. In addition, he also gives formulas for "dirty" bubbles. But, as he points out, for the dirty bubbles, the effective value of K would be reduced an unknown amount, casting doubt on its validity. In any case, the critical radii are lowered by the presence of a surface coating on the bubble, making upper bounds of the clean bubble estimates of critical radii.

3. BUBBLE GENERATION MECHANISMS

This chapter reviews briefly the research on the various bubble-generation mechanisms; details and implications of these results will be discussed in Ch. 4.

3.1 Surface-wave generation

The measurements of B & W pertain to surface waves breaking, although it is not clear whether the breaking is due to waves shoaling or due to the wind. Their measurements were made at a 10 cm depth near the beach with fresh winds on shore. There was a strong monotonic decrease in the number of bubbles as the radius increased through the range of measurements from 37 μm to 250 μm.

Glotov, et al (1972) have studied wave generation of bubbles in a 3 m deep tank at different laboratory-generated wind speeds. Both acoustic and optical determination of the bubble concentrations were made at a depth of 1.5 m. Their technique provided measurements of bubbles from 27 to 137 μm radius. They report that relatively few bubbles are formed at wind speeds of less than 10 m/s, while an abrupt increase in bubbles is observed for speeds of greater than 10 m/s, when whitecaps are formed. These wind speeds are not directly applicable to the open ocean, due to the restricted fetch in the laboratory. However, there may be some means of relating the measurements to open sea conditions.

Unfortunately, they do not report actual values of bubble concentrations, although they do describe a relative bubble concentration function vs radius. They further state that the shape of this function is almost independent of wind speeds for winds greater than 10 m/s.

As noted before, most of our present knowledge of bubbles in the sea comes from Medwin and his associates. For over a decade, they have been developing different methods of detection of bubbles and have been making ocean measurements, principally in coastal waters. Their measurements span depths from 1.5 to 15 m, radii from 18 to 180 μm and conditions from sea state one to winds of 14 m/s. Details of these works are given in Ch. 4. Their detection techniques include the use of acoustic absorption, scattering, and dispersion; optical techniques were used in earlier studies to verify the acoustic methods.

3.2 Precipitation — Rain, Snow and Dust

B & W have made laboratory measurements of bubble production of simulated rain to study the dependence of drop size on the generation of bubbles. They found that small drops (200 μm radius) will produce two or three 25 μm radius bubbles that are carried 1 to 3 mm below the surface. However, large drops (> 2000 μm radius) can produce well over 200 bubbles to depths of 2 to 4 cm. The vast majority of the bubbles are under 25 μm radius. They point out that the bubbles are formed by both the direct impact of the drop, and also by the splashed drops it creates.

B & W also found snow to be a significant factor in creating bubbles. From fifty to several hundred bubbles are produced by the melting of a single snowflake. Using a low-power microscope, they are able to produce a bubble-size distribution function. We have found that his function fits fairly well to

$$P(R) = \left(\frac{R}{b}\right) e^{-(R/a)^3}, \qquad \text{[Eq. 8]}$$

with $b = 50\ \mu m$, $a = 30\ \mu m$. $P(R)\Delta R$ is the probability of a bubble having a radius between R and $(R + \Delta R)$. During these measurements, they observed that bubbles with a radius smaller than 15 μm grew

smaller, while those greater than 25 μm grew larger, in agreement with the analysis of the Le Blond (1969). Therefore, P(R) will evolve with time, and Eq. 8 is only appropriate for times that are small compared with a bubble's lifetime.

Medwin (1970) has suggested that some of the bubbles he observed were due to either photosynthesis or continental dust carrying air into the water. The radii of these bubbles ranged from 18 μm (lower limit of observation) to 50 μm. He observes a reduction in their numbers at night. The question of origin of these bubbles is further discussed in Ch. 4.

3.3 Photosynthesis

LaFond and Dill (1952) have made measurements of various properties of a costal-water region, including oxygen content and turbidity. They take the oxygen supersaturated top layer as evidence for photosynthetic activity in the underlying turbid layer observed between 15 and 25 feet depth. However, the only direct evidence for bubbles comes from the observations of foam lines on the surface. They also point out that the origin of these bubbles could also be due to the following mechanism.

3.4 Heating of Saturated Waters

There is no direct measurements of bubbles formed by the heating of waters saturated with gas. However LaFond and Dill observed that foam was associated with coastal slicks and speculated that this might be due to this mechanism. On an annual basis, the waters give off air in the spring/summer seasons that was stored in the fall/winter months. If this gas is given off in the form of 25 μm bubbles, the flux would be 2500/cm^2/s through the surface (B & W), much longer than any bubble observations. Undoubtedly, most of the air exchange is due to molecular diffusion at the surface, but if strong heating occurs with weak or no vertical mixing, it is easily possible to form many bubbles.

3.5 Bubbles of Biological Origin

Although it is well known that bubbles are released by fish, quantitative estimates are lacking in the literature.

3.6 Bubbles due to Chemical Decomposition

McCartney and Barry (1965) report observations with an echo sounder of bubbles forming on a 200 m depth bottom. The size, inferred from the vertical velocity, was from 450 to 750 μm radius at the bottom, with a distribution of 85% between 550 to 600 μm. They further state that there were no bubbles produced at 50 and 300 μm radii. The bottom conditions were anaerobic, and therefore possibly

methane was the bubble gas. The actual volume fraction of gas in these waters due to these bubbles is about 3×10^{-15}, seven to ten orders of magnitude smaller than wave-generated bubbles near the surface.

3.7 Surface Emission by Bursting Bubbles

MacIntyre (1972) has studied some of the physics in breaking bubbles at the surface, showing that during millimetre-size bubble collapse, many small bubbles are injected back into the water. These bubbles ($< 50\,\mu m$ radius) are injected a centimetre or two below the surface, but then could be carried downward further by water motions. It is possible that the smallest bubbles measured by B & W at a 10 cm depth are due to this mechanism.

4. BUBBLE CONCENTRATIONS

4.1 Description Method

Although there are various ways of describing the bubble concentrations, we will follow the method of B & W and Medwin, using the units of Medwin. The basic function is the number of bubbles per cubic metre per micrometre (micron) increment of radius, $\psi(R)$, or "bubble spectrum". Multiplying this function by $4/3\pi R^3$ will yield the gas fraction volume per micrometre radius increment, and integrating this with respect to R from zero to infinity will yield the gas fraction volume due to all bubbles.

We write the total bubble concentration as a sum of the separate bubbles concentrations generated by the various mechanisms in the previous section.

$$\Psi = \Psi_W + \Psi_P + \Psi_{Ph} + \Psi_{SS} + \Psi_B + \Psi_C + \Psi_{SE} \qquad \text{[Eq. 9]}$$

where the subscripts W, P, Ph, SS, B, C, SE refer to the generating processes of waves, precipitation, photosynthesis, supersaturation, biological, chemical decomposition, and surface emission respectively. The individual bubble spectra are then discussed separately when possible.

4.2 Wave-inducted Bubble Concentrations, Ψ_W

Figure 2 shows the results of B & W at d = 10 cm depth, indicating that Ψ is consistent with an R^{-5} dependence up to about 300 μm radius. Although the data measured on the leeside of a rock can also be fitted to a R^{-5} function, we will not use it in

subsequent discussion. B & W state that its lower values may be due to either wind shielding by the rock, or due to a lower wind speed at the time of measurement. In either case, B & W seem to feel that their measurements of bubble concentration are dependent on the wind, rather than the shoaling and subsequent breaking of waves.

An example of Medwin's scatter derived data (1970) in Fig. 3 shows the sea-state dependence at a 10 ft depth. For bubbles smaller than 60 μm, the dependence is not evident. These bubbles are not believed to be due to waves and are left for later discussions. Figure 4 displays some of Medwin's absorption derived data, which have been multiplied by the volume of the bubble to produce the "fractional bubble volume spectrum". Bubbles smaller than 60 μm have a day/night dependence, while at the larger radii this dependence is not as striking. The R^1 dependence corresponds to an R^{-2} dependence in Ψ from 60 μm to 180 μm (upper limit of observations).

The result of tank experiments of Glotov et al (1962) are shown in Fig. 5. They state that the shape is independent of wind speed, W, for $W \geq 10$ m/s. This speed, at which the onset of whitecaps is noted, corresponds perhaps to 6 m/s in the open ocean when the same event occurs. To rationalize this shape with the measurements of Medwin and B & W requires some speculation. Although the region above 100 μm is consistent with B & W (R^{-5}), there is a lessening of slope and eventual decreasing of Ψ for smaller radii. It is possible that at the shallow depth of the measurements of B & W (10 cm) surface emission (Ψ_{SE}) also contributed to the small radii portion of Ψ. Since Medwin's 1970 data were measured at sea states 1 and 2, it is not expected that his shape would have "evolved" to that of Glotov et al. However, going from sea state 1 to 2, indicates a steepening of slope for $R > 100$ μm (Fig. 3) and may indicate that the spectrum is becoming more similar to that of Glotov as wind speeds increase.

In an attempt to assess the wind dependence of Ψ, we have tabulated some gas-volume fraction data (Table 1), mostly at 3 m depth (see Fig. 6). It appears that the differential speed method results in a different wind speed dependence than the other two methods. B & W's data may be extrapolated by the depth-dependence model described later. In addition, some of the value can be attributed to surface emission, Ψ_{SE}, but certainly no more than 50%. Finally an equivalent wind speed must be estimated, probably greater than 6 m/s but perhaps no more than 15 m/s. The resulting B & W estimate is still a factor of thirty higher than Medwin's (1975) 14 m/s value, and is more in agreement with the other values.

It is obvious that too few measurements exist to give an accurate estimate of wind-speed dependence. However, in the spirit of creating a simple model that describes the existing data, the following wind dependence is offered, which is consistent with estimating W = 12 m/s for the data of B & W with 1/3 of the volume fraction due to surface emission.

$$U(W) = AW^3 \qquad \text{[Eq. 10]}$$

where U is the volume fraction of gas, W is wind speed in m/s and $A = 3.7 \times 10^{-9} s^3/m^3$.

TABLE 1

VOLUME GAS FRACTION

Investigator	W(m/s)	u	Depth (m)
Medwin 1970 Absorption method	1	4.7×10^{-8}	3
Medwin 1970 Scattering method	1	4.0×10^{-8}	3
Medwin 1970 Scattering method	2	2.2×10^{-7}	3
Medwin 1975 Differential speed method	12-15	1.9×10^{-7}	3
B & W	?	1.7×10^{-5}	0.1
B & W Extrapolated to 3 m	?	1.1×10^{-5}	3
B & W Extrapolated to 3 m assuming 50% due to surface emission	?	5.5×10^{-6}	3

Equation 10 has the characteristics that U(0) = 0, while U(W) increases rapidly with W, as noted by Glotov. However, it may be in error both in form and value due to the crude estimates necessary for its establishment: again if the shape of Ψ is independent of W, then:

$$u \propto \Psi \propto W^3 .$$

Medwin reports a depth dependence proportional to $d^{-\frac{1}{2}}$ for iso-frequency measurements. However, the resonant frequency for $d > 10$ m has a $d^{-\frac{1}{2}}$ dependence, indicating perhaps no depth dependence of Ψ for a constant R. A simple, physically-tractable depth-dependence model would be for a well-mixed layer in which the lifetime of the bubbles,

$$\tau \gg \frac{d}{u} \quad \text{and} \qquad \text{[Eq. 11]}$$

$$u \gg w$$

where u is a characteristic water velocity, d is the depth, and w is the vertical velocity of the bubble. In this case, the radius of the bubble will have a depth dependence from the ideal gas law:

$$R(d) = \frac{R(0)}{(1+\frac{d}{10})^{\frac{1}{3}}} . \qquad \text{[Eq. 12]}$$

For example, Medwin's data would have a form

$$\Psi(R, d) = b(1 + \frac{d}{10})^{-\frac{2}{3}} R^{-2}$$

in the region of $60\,\mu m < R < 130\,\mu$. We have fitted his data to a R^{-2} dependence for each depth, calculating $\Psi(100\,\mu m)$ from the fit. The values of $\Psi(100)$ are plotted vs depth in Fig. 7, along with the prediction of Eq. 12. The fit seems reasonable for depths down to 25 ft, but for greater depths Ψ is higher than the model. If the assumptions of Eq. 11 are violated, then Ψ should be less than the prediction of a "well mixed" model, since some bubbles will be going into solution faster at the greater depths. A possible explanation is that there is a source of bubbles at depth possibly photosynthetic, increasing the population.

From the above discussions, the following model for $\Psi(R, W, d)$ is proposed:

$$\Psi_W(R,W,d) = C_1 W^3 (1+\frac{d}{10})^{-\frac{5}{3}} R^{-5} \qquad 80\,\mu m < R < 300\,\mu m$$

$$\Psi_W(r,W,d) = C_2 W^3 (1+\frac{d}{10})^{-\frac{1}{3}} R^{-1} \qquad 50\,\mu m < R < 80\,\mu m \qquad \text{[Eq. 13]}$$

which is a compromise between the spectrum shapes of B & W, Glotov, and Medwin. $C_1 = 9 \times 10^{10}$, $C_2 = 4.5 \times 10^1$, d in metres, W in m/s, R in micrometres and Ψ in bubbles per cubic metre per micrometre radius increment. For low W, the shape will not be in agreement with Medwin, and for $50\,\mu m < R < 80\,\mu m$, the slope is between B & W and Glotov, favouring Glotov, since we feel that the small bubbles close to the surface may be due to surface effects, and are accounted for in Ψ_{SE}.

4.3 Bubble Concentrations due to Photosynthesis, Ψ_{Ph}

Bubbles in the region $18\,\mu m < R < 50\,\mu m$ measured by Medwin (1970) are believed not to be due to waves but possibly to photosynthesis because they do not appear to have a sea-state dependence, and it appears that their source lies at depth. This conclusion comes from the following analysis. We have fitted data that he had converted to an equivalent radius, R', at the surface via Eq. 11 (Fig. 8) to an $(R)^{-4}$ form. Plotting the value of Ψ at $R' = 25\,\mu m$

vs depth (Fig. 9), we see that $\Psi(R')$ increases with depth. Since the pressure effect has been taken into account by referring the radius to the surface, the increase in $\Psi(R')$ with depth means an increase of the mass of gas with depth, indicating a generation of gas at depth.

Although there does not seem to be a depth dependence in $\Psi(R)$ (see Fig. 4), possibly due to the balancing effects of the pressure effects [Eq. 11] and the positive gradient of the mass of the gas, there is a pronounced diurnal effect, which would be expected in photosynthetic activity. The model that best fits this data is:

$$\Psi_{Ph}(R, t) = C_3 t R^{-4} \qquad \text{[Eq. 14]}$$

where $t = 1$ during the night and 2 during the day. $C_3 = 1.6 \times 10^9$, but must vary considerably from location to location. In particular, away from coastal areas, C_3 might be much lower, and Eq. 14 may even take on a different form.

4.4 "Surface Emission" Bubble Concentration, Ψ_{SE}

From the discussion of Ψ_W, it was concluded that the excess of Ψ as measured by B & W would be accounted for by Ψ_{SE}. It is quite possible that these bubbles are due to a strong depth dependence for small bubbles and not due to "surface emission". However, at this stage there is no way to distinguish the process; so, for convenience, we are including them here. In addition, there is no depth information. Since we expect these bubbles to exist only near the surface, we will make an exponential dependence. Although this is quite arbitrary, to be consistent with Glotov, we need to have essentially no bubbles at his depth of measurements of 1.5 m. We therefore write

$$\Psi_{SE} = C_4 W^3 \left(1 - e^{-\frac{d_1}{d}}\right) R^{-5} \qquad 35\,\mu m < R < 80\,\mu m \qquad \text{[Eq. 15]}$$

with $C_4 = 2.7 \times 10^{11}$, chosen so that $\Psi_{SE} = \Psi_W$ at 80 μm at 0.1 m depth. $d = 0.03$ is chosen from the comments of McIntyre (1972).

CONCLUSIONS

Vertical velocity predictions seem to be fairly well established, although there may be some uncertainty due to the surface coatings of the bubbles. Lifetimes and growth predictions may be applicable for small, clean bubbles, but large uncertainties arise when the bubble has a film or coating, and when the radius of the bubble is greater than about 80 micrometres. The bubble concentration spectrum, (the number of bubbles per cubic metre per micrometre radius increment) is written as:

$$\Psi = \Psi_W + \Psi_P + \Psi_{Ph} + \Psi_{SS} + \Psi_B + \Psi_C + \Psi_{SE},$$

where the subscripts W, P, Ph, SS, B, C and SE refer to the bubble-generating mechanisms of waves, precipitation, photosynthesis, supersaturation, biological, chemical decomposition and "surface emission", respectively. Due to scarcity of data, we have attempted to model only Ψ_W, Ψ_{Ph} and Ψ_{SE}, and we must expect only rough correspondence between these models and actual data. From one observation, it appears that Ψ_C may be very small, and negligible near the surface. It is possible that Ψ_{SS}, production of gas due to heating of supersaturated water, on the other hand, may be important, but we have no information regarding this mechanism. Information of the wind dependence of Ψ_W is scant but very important to predicting Ψ. Certainly the most important aspect to be studied in the future is this wind dependence.

PART 2 BUBBLES CONTAINED IN LIVING ORGANISMS

INTRODUCTION

Since free bubbles have been discussed in some detail, it is now necessary to review the other class of bubble population in the sea — those associated with living organisms. Since the discovery of the deep scattering layer (DSL) in the 1940's [Hersey and Backus, 1962], its cause has been examined by many workers and the conclusions reached showed that it was of biological origin. Marshal [as outlined in Hersey and Backus, 1962] listed the requirements for a living organism to be responsible for the DSL — a widely distributed organism, powers of diurnal migration, sufficient concentration, and the ability to reflect sound. Two types of organisms have been shown to qualify: myctophids (also called lantern fish) [Hersey and Backus, 1962] and siphonophores (a colony of jellyfish) [Barham 1963]. The sound scattering ability of these organisms comes from associated gas bubbles that resonate at acoustic frequencies. Other hard shelled organisms have been proposed but are not discussed here since they do not contain gas bubbles.

Historically, this subject has been reviewed by Hersey and Backus [1962] in volume 1 of The Sea, a theoretical article by Weston [1967] and, most recently, by many authors in a symposium held in 1970 [Farquhar, 1970] entitled "Biological Sound Scattering in the Ocean".

In this part it is proposed to discuss the two principal types of animals involved in sound scattering and put forward some relations that may be used to model their size and distribution.

1. MYCTOPHIDS

The greater number of articles discussing this problem refer to myctophids as the main component of the DSL [Dietz, 1962; Backus et al, 1968; Batzler and Pickwell, 1970] — these are fish with lengths of 2 to 20 cm containing a gas bladder in the shape of a prolate spheroid. Marshall [1970] has studied the biology of these fish in great detail. The bladder is believed to be used to aid in the diurnal migration of the fish but its exact mode is yet to be determined [Alexander, 1970; D'Aoust, 1970]. Some fish appear to use it in the "passive" mode in which as the fish ascends or descends, the bubble expands or contracts following the gas law. The fish is believed to be in equilibrium at its upper depth limit and must expend energy at its lower limit to maintain a constant level. The other mode of operation is the "active" one in which the fish maintains the bladder at constant size during migration, creating or absorbing gas as required. Both types of operation have been inferred from acoustic results and the resolution of the problem is still an open question. For modelling purposes, the size of the swimbladder is important, along with the density of the fish population. The size of the swimbladder as related to the size of the fish has been the study of many and a summary of is available [Shearer, 1970]. There are various methods of determining volume [Shearer, 1970] which will not be discussed here but, in general, the end result is to try to obtain a relationship of the form

$$V = KL^n \qquad \text{[Eq. 16]}$$

where V is the volume of the swimbladder, K and n are the constants, and L is the length of the fish. An order-of-magnitude relationship is of the form with $K = 5 \times 10^{-4}$ and $n = 3$.

Figure 10 shows the results from Shearer [1970] where the estimated swimbladder volume is plotted against the length of the fish for four different fish. The dotted lines are the lines as fitted by Shearer [1970] but it was felt after examination that they did not adequately fit the data points. A new least-squares fit was calculated for the points, using the criterion that the square of the distance from each point to the line should be minimized [instead of the ordinate distance squared that Shearer (1970) used.] It can be seen from Fig. 10 that a steeper slope resulted without a consistent value, but was certainly higher than the commonly used 3. We tested further data from Holliday (1972] and the results can be seen in Fig. 11. The data here were in the form of histogram distributions of number of fish with given lengths and other distributions of bubble size. We assumed a one-to-one correspondence between smaller fish and smaller bubble volume to get the points on the figure — deviations from this assumption would tend to give a steeper slope. The conclusion reaches is that different values of K and n need to be used for different species, but almost all values of n were greater than 3.

As for the observed size distribution of scatterers of the myctophid type, Van Schulyer [1970] reported on this for both day and night time observations north of Hawaii. He calculated the effective radius of swimbladder and the number of scatterers per cubic metre reported, with the numbers varying from 3×10^{-3} to $3 \times 10^{-8}/m^3$. We converted these data to the same units as reported for free bubbles (number of bubbles/m^3 in a one micrometre bandwidth) and the results are shown in Fig. 12. It can be seen that the slope of the line is -5.5 which is about the same as that observed for free bubbles but with a much lower density of population. The day and night distributions were about the same. These were the only data that gave the size distribution, but other reports [Andreyeva, 1972; Johnson, 1973; Hersey and Backus, 1962] give values of total concentration that range from 4×10^{-4} to $2.4 \times 10^{-3}/m^3$. In schools, values of 10 to 15/m^3 have been reported with school sizes of 5 to 10 m wide by 10 to 100 m long, and being about 100 to 200 m apart.

2. SIPHONOPHORES

The other class of biological organisms that contains associated bubbles is the siphonophore, a jelly fish that contains a bubble at its apex that is used for flotation purposes [Barham, 1963; Pickwell, 1967]. The size of these bubbles vary from 0.03 to 2.51 mm^3 and it has been noted that these organisms can expel bubbles, thus being a source (Ψ_B) of free bubbles in the ocean. Populations of 0.3/m^3 have been noted [Barham, 1963] in a visual observation.

CONCLUSIONS

Resonant scattering from biological organisms is believed to be caused either by the gas bladder of myctophid fishes or the flotation bubble of siphonophores, with the greater work being concentrated on the former. No simple relationship exists to compute the volume of the bladder of fishes but rough estimates can be made from power law relationships. The density of population of fishes can vary by orders of magnitude whether or not a school is present, and there is no scheme proposed to date for this prediction.

REFERENCES AND BIBLIOGRAPHY

ALEXANDER, R. McN. Swimbladder gas secretion and energy expediture in vertical migrating fishes. In FARQUHAR, G.B. 1970: 74-85.

ALLEN, H.S. The motion of a sphere in a viscous fluid. Philosophical Magazine 50, 1900: 323-338.

ANDERSON, A.L., HARWOOD, R.J., LOVELACE, R.T. Investigation of gas in bottom sediment, ARL-TR-70-28. Applied Research Laboratories, The University of Texas at Austin, 1971.

ANDREYEVA, I.B. The nature of scatterers and frequency characteristics of sound scattering layers in the ocean. Oceanology 12(6) 1972: 818-822.

BACKUS, R.H., CRADDOCK, J.E., HAEDRICH, R.L., SHORES, D.L., TEAL, J.M., WING, A.S., MEAD, G.W. and CLARKE, W.D. Ceratoscopelus maderensis: peculiar sound-scattering layer identified with this Myctophid fish. Science 160, 1968: 991-993.

BARHAM, E.G. Siphonophores and the deep scattering layer. Science 140, 1963: 826-828.

BATZLER, W.E. and PICKWELL, G.V. Resonant acoustic scattering from gas-bladder fishes. In FARQUHAR 1970: 168-179.

BLANCHARD, D.C. and WOODCOCK, A.H. Bubble formation and modification in the sea and its meteorological significance. Tellus 9, 1957: 145-158.

BUXLEY, S., MCNEIL, J.E., MARKS, R.H. Jr. Acoustic detection of micro-bubbles and particulate matter near the sea surface, NPS 50306. Monterey, Calif., Naval Postgraduate School.

D'AOUST, B.G. Physiological constraints on vertical migration by Mesopelagic fishes. In FARGUHAR, G.B. 1970: 86-99.

DATTA, R.L., NAPIER, D.H. and NEWITT, D.M. The properties and behavior of gas bubbles formed at a circular orifice. Trans. Institution Chemical Engineers 23, 1950: 14-26.

DEVIN, C. Jr. Survey of thermal, radiation, and viscous damping of pulsating air bubbles in water. Jnl Acoustical Society America, 31, 1959: 1654-1667.

DIETZ, R.S. The sea's deep scattering layers. Oceanography, Freeman, San Francisco, 1962.

DORSEY, N.E. Properties of Ordinary Water Substance. New York: Reinhold, 1940.

FARQUHAR, G. Bruce (ed.). Proceedings of an International Symposium on Biological Sound Scattering in the Ocean. MC Report 005. Washington D.C., U.S. Govt. Printing Office, 1970.

FEIN, M. and MANGULIS, V. The acoustic pressure scattered by a finite number of bubbles. TRG, Inc. Report No. 023-TN-66-26, Melville N.Y. 1966.

FITZGERALD, James. Statistical study of sound speed in the inhomogeneous upper ocean, M.S. thesis. Monterey, Calif., Naval Postgraduate School, 1972.

GARRETTSON, G.A. Bubble transport theory with application to the upper ocean. Jnl Fluid Mechanics 59, 1973: 187-206. [Also Naval Postgraduate School, 6 April 1973, AD 761999].

GAVRILOV, L.R. On the size distribution of gas bubbles in water. Soviet Physics-Acoustics 15, 1969: 22-24.

GIBSON, F.W. Measurement of the effect of air on the speed of sound in water. Jnl Acoustical Society America, 48, 1970: 1195-1197.

GLOTOV, V.P., KOLOBAEV, P.A., NEUIMIN, G.G. Investigation of the scattering of sound by bubbles generated by an artificial wind in sea water and the statistical distribution of bubble sizes. Soviet Physics Acoustics 7, 1962: 341-345.

GLOTOV, V.P. and LYSONOV, Y.P. Influence of a nonuniform distribution of air bubbles on the reflection of sound from the surface layer of the ocean. Soviet Physics Acoustics 11, 1966.

GOLDSTEIN, S. Modern Developments in Fluid Dynamics, Vol 1. Oxford, The University Press, 1938: p.14.

HARTUNIAN, R.A. and SEARS, W.R. On the instability of small gas bubbles moving uniformly in various liquids. Jnl Fluid Mechanics 3, 1957: 27-47.

HERSEY, J.B. and BACKUS, R.H. Sound scattering by marine organisms. In HILL, M.N. The Sea, New York, Interscience, 1962.

HIESTAND, F.H. Bubble distributions in the upper ocean. Monterey, Calif., Naval Postgraduate School, 1971. [AD 738968].

HOLLIDAY, D.V. Resonance structure in echoes from schooled pelagic fish. Jnl Acoustical Society America 51, 1972: 1322-1332.

JOHNSON, R. Frequency dependence of the daily pattern of sea reverberation. Jnl Acoustical Society America 54, 1973: 478-482.

KELLER, D.G. Evaluation of a standing wave system for determining the presence and acoustic effect of microbubbles near the sea surface, M.S. thesis. Monterey, Calif., Naval Postgraduate School, 1968.

LAFOND, E.C. and DILL R.F. Do invisible bubbles exist in the sea. Tech. Memo. TM-259. San Diego, Calif., U.S. Navy Electronics Lab., 1957.

LEBLOND, P.H. Gas diffusion from ascending gas bubbles. Jnl Fluid Mechanics 35, 1969: 711-719.

LEIBERMAN, L. Air bubbles in water. Jnl Applied Physics 28, 1957.

MACINTYRE, F. Flow patterns in breaking bubbles. Jnl Geophysical Research 77, 1972: 5211-5228.

MACINTYRE, F. The top millimeter of the ocean. Scientific American 230, 1974: 62-77.

MARSHALL, N.B. Swimbladder development and the life of deep sea fishes. In FARQUHAR, G.B. 1970: 69-73.

MCCARTNEY, B.S. and BARRY, B.M. Echosounding on probable gas bubbles from the bottom of Saanich Inlet, British Columbia. Deep Sea Research 12, 1965: 285-294.

MEDWIN, H. In-situ acoustic measurements of bubble populations in coastal ocean waters. Jnl Geophysical Research 75, 1970: 599-611.

MEDWIN, H. The rough surface and bubble effect on sound propagation in surface ducts. Tech. Rpt. NPS-61Md71101A. Monterey, Calif., Naval Postgraduate School, 1971.

MEDWIN, H. Sound speed dispersion and fluctuations in the upper ocean: Project Bass. NPS-61Md73101A, Monterey, Calif., Naval Postgraduate School, 1973.

MEDWIN, H. Acoustic fluctuations due to microbubbles in the near-surface ocean. Jnl Acoustical Society America 56, 1974: 1100-1104.

MEDWIN, H., FITZGERALD, J. and RAUTMANN, G. Acoustic microprobing for ocean microstructure and bubbles. Jnl Geophysical Research 80, 1975: 405-413.

PICKWELL, G.V. Siphonophores and their released bubbles as acoustic targets within the deep scattering layer. In 4th US Navy Symposium on Military Oceanography, Vol I. Washington, D.C., Naval Research Laboratory, 1967: 383-395.

RAUTMANN, R. Sound dispersion and phase fluctuations in the upper ocean. NPS-61Md72022A. Monterey, Calif., Naval Postgraduate School, 1972.

SCHULKIN, M. Surface-coupled losses in surface sound channels. Jnl Acoustical Society America 44, 1968: 1152-1154.

SCHULKIN, M. Surface-coupled losses in surface sound channel propagation. II. Jnl Acoustical Society America 45, 1969: 1054-1055.

SCHULKIN, M. The propagation of sound in imperfect ocean surface ducts. U.S.L. Report No. 1013. New London, Conn., U.S. Navy Underwater Sound Laboratory, 1969.

SHEARER, L.W. Comparisons between surface-measured swimbladder volumes, depth of resonance and 12 kHz echograms at the time of capture of sound-scattering fishes. In FARQUHAR, G.B. 1970: 453-473.

TOBA, Y. and KUNISHI, H. Breaking of wind waves and the sea surface wind stress. Jnl Oceanographical Society of Japan 26, 1970: 71-80.

TURNER, J.S. Buoyancy effects in fluids. Cambridge, The University Press, 1973: 474-481.

TURNER, W.R. Microbubble persistence in fresh water. Jnl Acoustical Society America 33, 1961: 1223-1232.

URICK, R.J. and HOOVER, R.M. Backscattering of sound from the sea surface: its measurement, causes, and application to the prediction of reverberation levels. Jnl Acoustical Society America 28, 1956: 1038-1042.

VAJDA, T.C. Bubble distributions in a quiescent ocean calculated from the bubble transport equation. Monterey, Calif., Naval Postgraduate School, 1972. [AD 749046].

VAN SCHULYER, P. An acoustically determined distribution of resonant scattering north of Oahu. In FARQUHAR, G.B. 1970: 328-340.

WANG, P.C.C. and MEDWIN, H. Statistical considerations to experiments on the scattering of sound by bubbles in the upper ocean. NPS-53Wg72101A, Monterey, Calif., Naval Postgraduate School, 1972.

WESTON, D.E. Underwater Acoustics, Vol 2, Ch 5. In ALBERS. V.M. (ed.) Sound propagation in the presence of bladder fishes. New York, Plenum Press, 1967.

WIENS, L.A. Development and testing of an acoustic system for in-situ determination of microbubble concentrations in the ocean. Monterey, Calif., Naval Postgraduate School, 1971. [AD 72869].

WYMAN, J. Jr., SCHOLANDER, P.F. EDWARDS, G.A. and IRVING, L. On the stability of gas bubbles in sea water. Jnl Marine Research 11, 1952: 47-62.

ZIMDAR, R.E., BARNHOUSE, P.D., and STOFFEL, M.J. Instrumentation to determine the presence and acoustic effect of microbubbles near the sea surface, M.S. thesis. Monterey, Calif., Naval Postgraduate School, 1964.

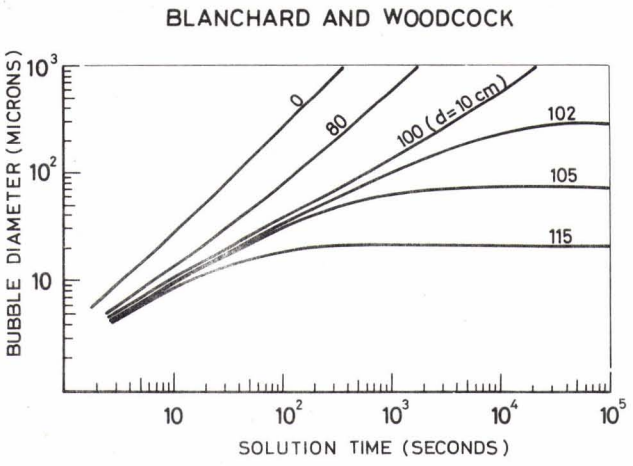

FIG. 1
BUBBLE LIFETIMES

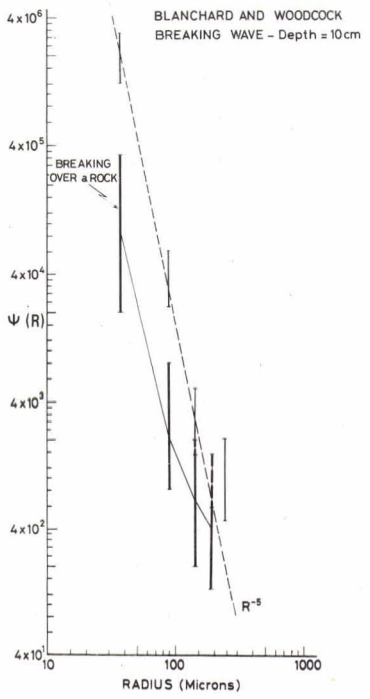

FIG. 2
BUBBLE SPECTRUM – BLANCHARD AND WOODCOCK

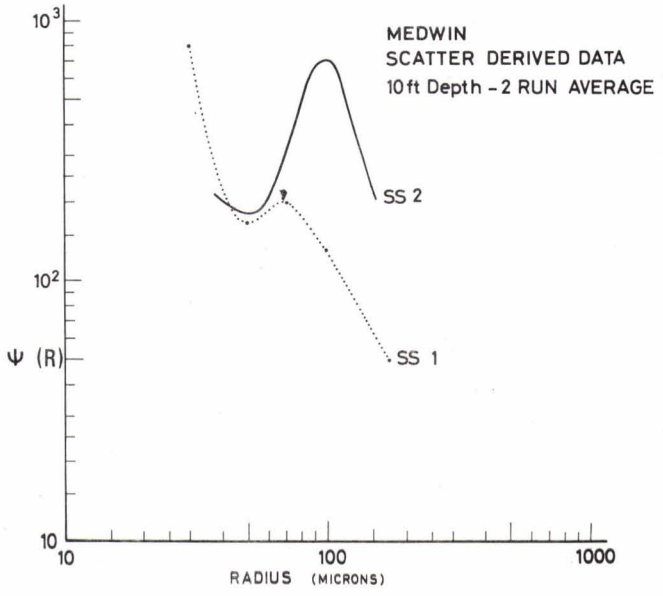

FIG. 3
BUBBLE SPECTRUM – MEDWIN

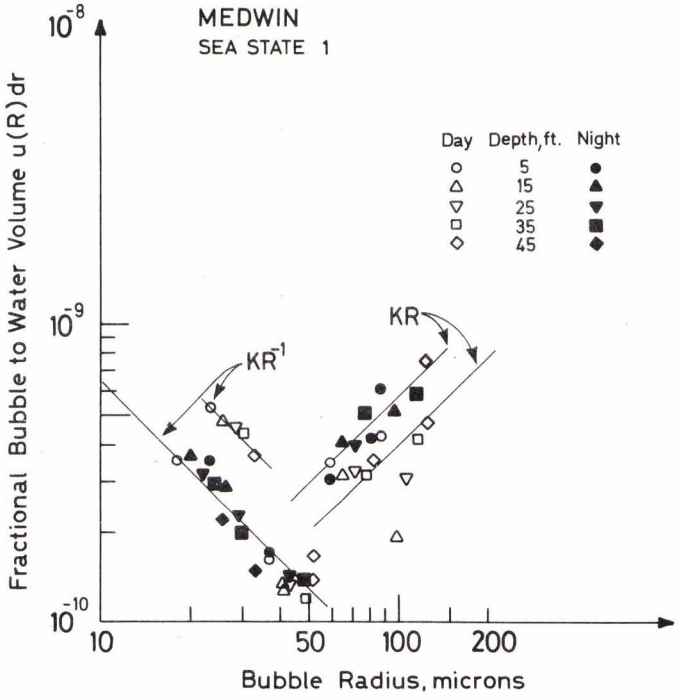

FIG. 4
'FRACTIONAL VOLUME' SPECTRUM – MEDWIN

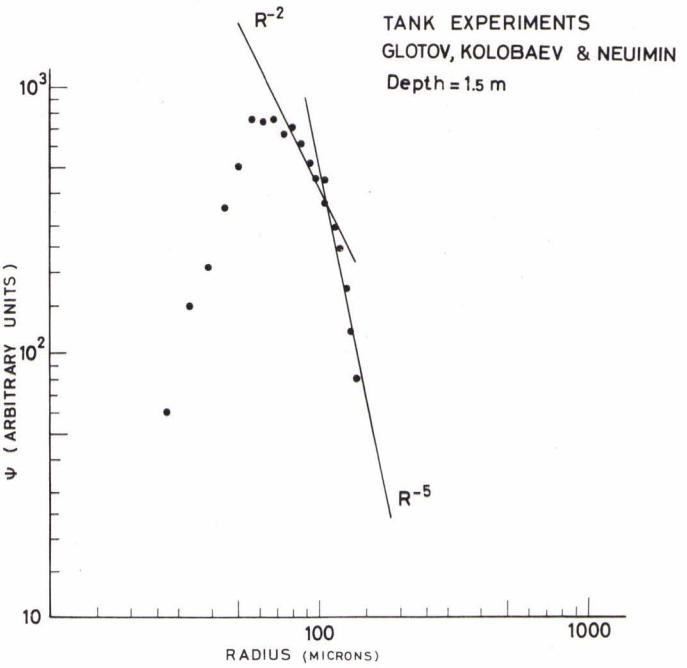

FIG. 5
BUBBLE SPECTRUM – GLOTOV

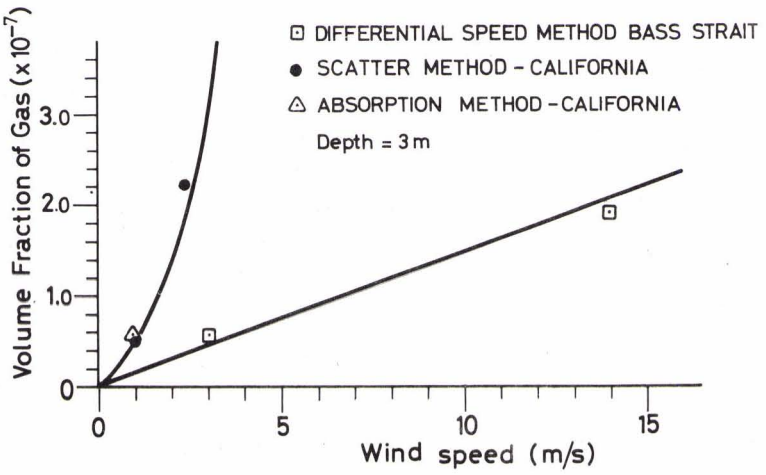

FIG. 6
BUBBLE WIND DEPENDENCE

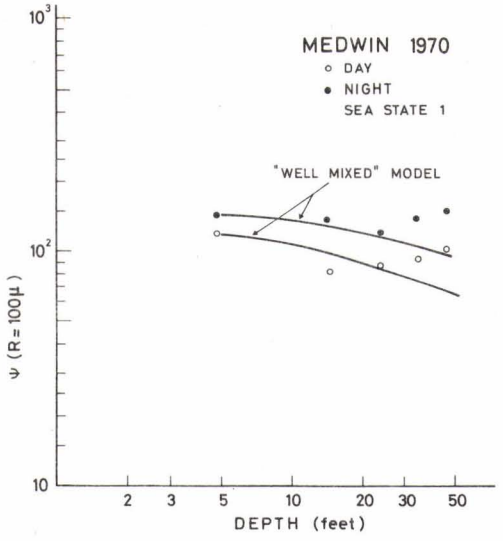

FIG. 7
BUBBLE DEPTH DEPENDENCE

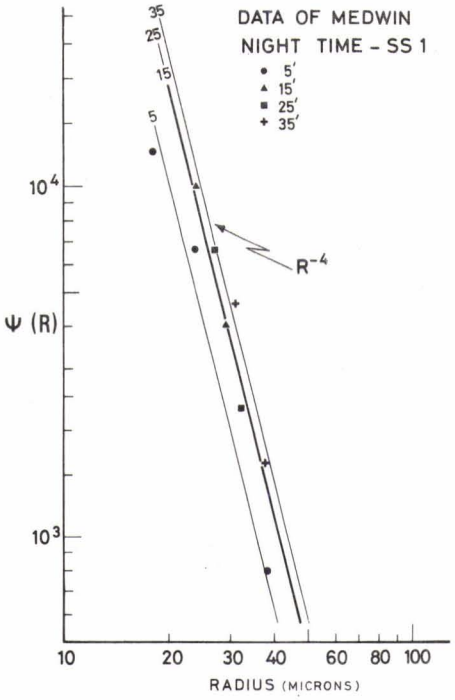

FIG. 8
ISOFREQUENCY DEPTH DEPENDENCE

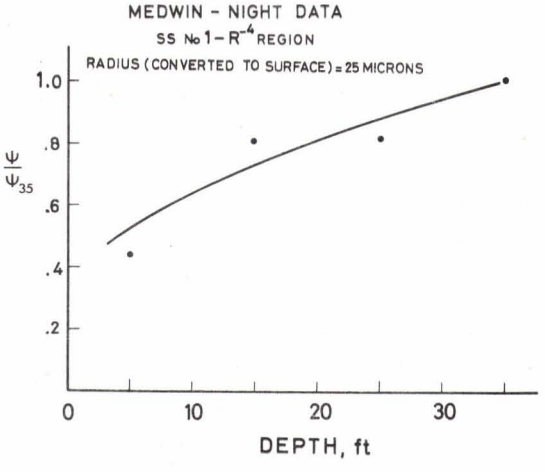

FIG. 9
DEPTH DEPENDENCE AT CONSTANT RADIUS

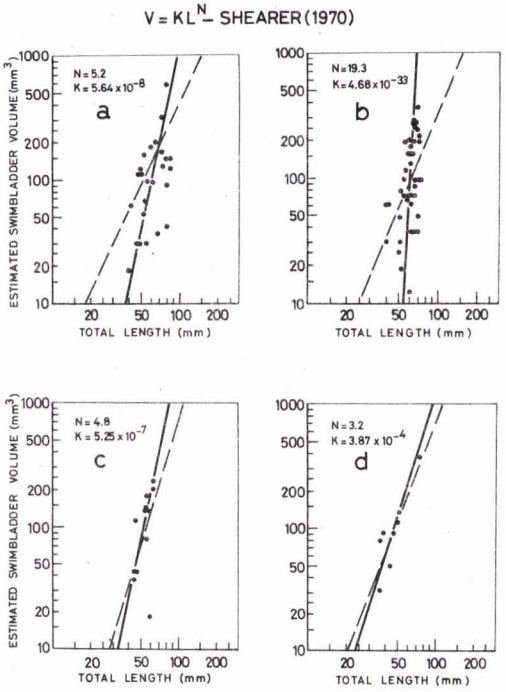

FIG. 10
ESTIMATED SWIMBLADDER VOLUME – VS FISH LENGTH
a Myctophum Nitidulum (surface)
b Lepidophanes Güntheri 0 – 230 m
c Diaphus Brachycephalus 230 – 0 m
d Sternoptyx Diaphana 860 – 0 m

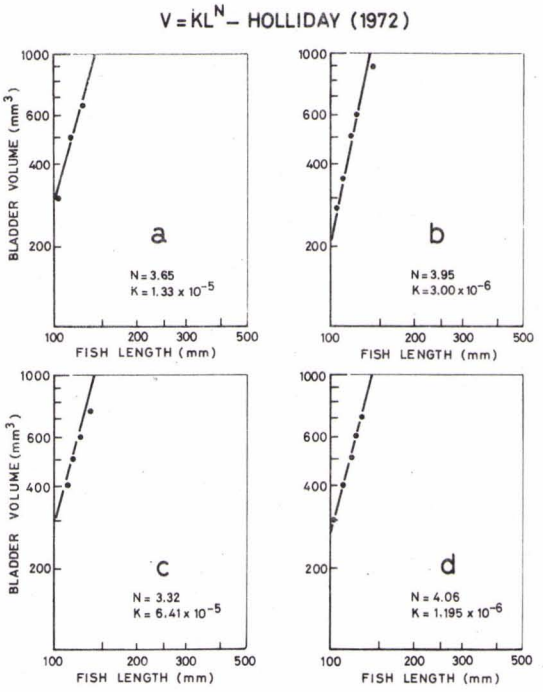

FIG. 11
ESTIMATED SWIMBLADDER VOLUME – VS FISH LENGTH
Anchovy

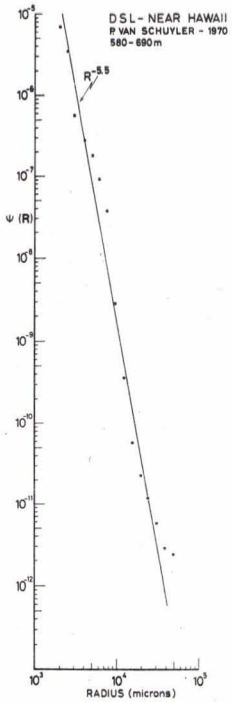

FIG. 12
BUBBLE SPECTRUM FOR A DEEP SCATTERING LAYER